

**SYNTHESIS OF SILICA AND CARBON
NANOPARTICLES FROM RICE HUSKS FOR
LATENT FINGERMARKS APPLICATION**

REVATHI A/P RAJAN

UNIVERSITI SAINS MALAYSIA

2018

**SYNTHESIS OF SILICA AND CARBON
NANOPARTICLES FROM RICE HUSKS FOR
LATENT FINGERMARKS APPLICATION**

By

REVATHI A/P RAJAN

Thesis submitted in fulfilment of the requirements

for the Degree of

Doctor of Philosophy

August 2018

ACKNOWLEDGEMENTS

My first and foremost gratitude goes to my main supervisor Dr. Nik Fakhuruddin Nik Hassan who gave me the opportunity to further my studies and who has been a pillar of strength and encouragement behind the successful completion of my research work. His skilled guidance was an invaluable asset that has inspired and motivated me to achieve beyond my expectations throughout this research. My extended gratitude to my co-supervisors, Dr. Yusmazura Zakaria and Professor Dr. Shaharum Shamsuddin who also contributed their part in guiding and aiding throughout the research work.

I am also extremely thankful to my family especially my father who supported me throughout my studies and enabled me to achieve my dream. My cousins and friends who also encouraged me through many difficult times and became my life coach. They guided me to look at the bright side and helped me to manage the stress throughout the studies.

My research work would not have been completed timely without the instrumental help from the entire staff of School of Health Science of Universiti Sains Malaysia especially Unit Kemudahan Makmal and Forensic Laboratory staffs. They were so kind, helpful and accommodating to aid any requests put forth. I am grateful to Universiti Sains Malaysia for providing RUI grant (1001/PPSK/812125) and MyBrain scholarship without which I could never have completed this research work.

I realise I am just a small part that contributed to the completion of this research and made whole by all the people who stood by me and helped me throughout this research journey. I am entirely grateful to everyone who was there for me at all the time of need. I dedicate my success to be shared by all that I would forever hold close to my heart.

TABLE OF CONTENTS

ACKNOWLEDGEMENTS	ii
TABLE OF CONTENTS	iii
LIST OF TABLES	xii
LIST OF FIGURES	xiv
LIST OF ABBREVIATIONS	xxx
ABSTRAK	xxxii
ABSTRACT	xxxiv
CHAPTER 1- INTRODUCTION	1
1.1 Research background	1
1.2 Fingermarks and forensic investigations.....	2
1.3 Problem statement.....	3
1.4 Aim and objectives.....	8
1.5 Scope of research	9
1.6 Thesis outline	10
CHAPTER 2- LITERATURE REVIEW	11
2.1 Nanoparticles.....	11
2.1.1 Nanoparticle synthesis	12
2.1.2 Nanomaterial characterisations.....	14
2.2 SiNP.....	15
2.2.1 SiNP synthesis	19

2.2.1 (a)	Extraction of SiNP through thermal decomposition of RH.....	21
2.2.1 (b)	Extraction of SiNP through precipitation	26
2.2.1 (c)	Extraction of SiNP through bio-organism transformation	36
2.3	Carbon nanoparticle.....	36
2.3.1	CNP synthesis.....	37
2.3.1 (a)	Acid assisted synthesis	39
2.3.1 (b)	Ultrasonification assisted synthesis.....	40
2.3.1 (c)	Thermal assisted synthesis	40
2.3.2	Hydrochars and activated carbon synthesis.....	41
2.4	Natural dyes	42
2.4.1	Curcumin	43
2.4.2	Carotenoids	43
2.4.3	Anthocyanin.....	45
2.4.4	Phycocyanin.....	46
2.5	Fingerprint and fingermark	47
2.5.1	Origin of fingermarks	48
2.6	Fingermarks and forensics	49
2.6.1	Identification using fingermarks	49
2.6.2	Sources of fingermarks residue	50
2.6.3	Factors affecting fingermark composition.....	53
2.6.3 (a)	Surface containing the fingermarks.....	53

2.6.3 (b)	Conditions of fingerprint deposition.....	54
2.6.3 (c)	Donor variations	54
2.6.3 (d)	Ageing	55
2.6.3 (e)	Environmental insults	57
2.6.3 (f)	Contaminants	58
2.7	Fingerprint development techniques	58
2.7.1	Powder dusting method	59
2.7.1 (a)	Regular powder	61
2.7.1 (b)	Magnetic and metallic powder	62
2.7.1 (c)	Luminescent powders	63
2.7.1 (d)	Powder application techniques	64
2.7.2	Physical staining	68
2.7.3	Chemical fuming techniques	69
2.7.4	Chemical treatment	70
2.7.5	Nanoparticle-based reagents	70
2.7.5 (a)	Metal nanoparticles techniques	70
2.7.5 (b)	Metal oxide and SiNP techniques.....	74
2.7.5 (c)	Quantum Dots (QD)	75
2.8	Summary	76
CHAPTER 3- THE SYNTHESIS OF SiNPs.....		78
3.1	Materials.....	78
3.2	Synthesis of nanoparticle WP	78

3.2.1	Flowchart	78
3.2.2	RHA preparation.....	80
3.2.3	Preparation of SS _{rh} solution	81
3.2.4	Precipitation of SiNP	81
3.3	Characterisation studies of the intermediates and final powder.....	84
3.3.1	Characterisation of RHA intermediates	84
3.3.1 (a)	Inductively Coupled Plasma Mass Spectrophotometer (ICPMS) analysis.....	84
3.3.1 (b)	FTIR	84
3.3.1 (c)	FESEM	85
3.3.1 (d)	EDS.....	85
3.3.1 (e)	XRD analysis.....	85
3.3.2	Characterisation of SiNP powders	85
3.3.2 (a)	FESEM	86
3.3.2 (b)	High Resolution Transmission Electron Microscope (HRTEM) analysis.....	86
3.3.2 (c)	Surface area and porosity measurements	86
3.3.2 (d)	Photoluminescence study of the SiNP _{sp} powder and fingerprint developed.....	87
3.4	Results and discussion	87
3.4.1	Silica extraction and SiNP synthesis	87
3.4.1 (a)	Purified RHA.....	87

3.4.1 (b)	Formation of SS _{rh}	88
3.4.1 (c)	SiNP formation.....	90
3.4.2	Characterisation studies of the intermediates and final powders.....	106
3.4.2 (a)	Characterisation of RHA intermediates.....	106
3.4.2 (b)	Characterisation of nanoparticle powders	115
3.5	Conclusions	130
CHAPTER 4- APPLICATION OF SiNP FOR LATENT FINGERMARK		
DEVELOPMENT		132
4.1	Materials.....	132
4.2	Methods	132
4.2.1	Determination of optimal SiNP powder for the development of latent fingerprint.....	132
4.2.2	Establishing interaction between the fingerprint and the SiNP	133
4.2.2 (a)	Surface testing using the synthesised fingerprint powder	133
4.2.2 (b)	Surface testing using wet powder suspension (NPR).....	136
4.2.2 (c)	Fingerprint grading	136
4.2.2 (d)	Statistical analysis	138
4.3	Results and discussion	138
4.3.1	Optimum SiNP size for latent fingerprint development	138
4.3.2	Application of SiNP as a dry dusting powder	142

4.3.2 (a)	Phase 1: Establishing the interaction of SiNP _{sp} powder and fingerprint residue	142
4.3.2 (b)	Phase 2: SiNP _{sp} powder sensitivity determination studies	148
4.3.3	Application of SiNP as wet powder suspension for fingerprint development.....	168
4.3.4	Interaction of SiNP with fingerprint residue	178
4.3.5	Previous reported studies on WP and reagents	180
4.4	Conclusions	184
CHAPTER 5- FORMULATION AND APPLICATION OF MULTICOLORED SiNPs FOR LATENT FINGERMARK DEVELOPMENT		
		186
5.1	Materials.....	186
5.2	Methods	187
5.2.1	Natural pigments extraction.....	187
5.2.1 (a)	Curcumin extraction from turmeric.....	187
5.2.1 (b)	Carotenoids extraction from red chillies	188
5.2.1 (c)	Blue anthocyanin extraction from butterfly pea flower .	188
5.2.1 (d)	Purple anthocyanin extraction from purple cabbage	189
5.2.1 (e)	Phycocyanin from spirulina tablets	189
5.2.2	Synthetic dyes	190
5.2.3	Characterisation of dyes	190
5.2.3 (a)	UV-Vis Spectroscopy	190

5.2.3 (b)	Photoluminescence study	190
5.2.4	Physical incorporation of dyes with SiNP	190
5.2.4 (a)	Direct mixing of SiNP powder with dye	191
5.2.4 (b)	Dyeing SiNP with cornstarch	191
5.2.4 (c)	Determination of optimal SiNP powder to cornstarch ratio.....	191
5.2.4 (d)	Production of dyed SiNP powders	191
5.2.5	Characterisation of the dyed SiNP powders	192
5.2.6	Application of dyed SiNP to develop fingerprints.....	193
5.3	Results and discussion	194
5.3.1	Natural pigment extraction	194
5.3.2	Characterisation of dyes	194
5.3.3	Physical incorporation of dye with SiNP.....	197
5.3.3 (a)	Direct mixing of SiNP powder with dye	197
5.3.3 (b)	Multicoloured SiNP powder produced with cornstarch addition.....	198
5.3.3 (c)	Production of dyed SiNP powders	199
5.3.4	Characterisation of dyed powders	200
5.3.5	Application of dyed SiNP to develop fingerprints.....	206
5.4	Conclusions.....	212
CHAPTER 6- SYNTHESIS AND APPLICATION OF CNP FOR LATENT FINGERMARK DEVELOPMENT.....		213

6.1	Materials	214
6.2	Methods	214
6.2.1	Synthesis of CNP powder through a top-down approach.....	214
6.2.1 (a)	Preparation of RH.....	214
6.2.1 (b)	Acid treatment	214
6.2.1 (c)	Alkali treatment	215
6.2.1 (d)	Removal of silica from treated RH.....	215
6.2.2	Synthesis of CNP powder via the bottom-up approach.....	216
6.2.3	Characterisation of CNP powders	217
6.2.3 (a)	FESEM	217
6.2.4	Establishing interaction between the fingerprint and the CNP powder	218
6.2.4 (a)	Surface testing using the synthesised fingerprint powder	218
6.2.4 (b)	Fingerprint grading and statistical analysis	221
6.3	Results and discussion	221
6.3.1	CNP powder via top down approach	221
6.3.2	CNP powder via bottom-up approach	223
6.3.3	Characterisation of CNP powder from bottom-up approach.....	226
6.3.4	Investigating the interaction and efficiency of the CNP ₁₈ powder in developing latent fingerprints	232

6.3.4 (a) Phase 1: Establishing interaction of CNP ₁₈ powder and fingerprint residue.....	232
6.3.4 (b) Phase 2: CNP ₁₈ powder sensitivity determination studies	237
6.3.5 Interaction of CNP with fingerprint residue	257
6.3.6 Previous reported studies on BP	257
6.4 Conclusions	259
CHAPTER 7- CONCLUSIONS	262
7.1 Conclusions	262
7.2 Limitations.....	264
7.3 Future studies.....	264
REFERENCES.....	266
APPENDICES	

Appendix A - Novelty search report by PINTAS

Appendix B - Product Evaluation by Royal Malaysian Police, Forensic
Laboratory, RMP Institute, Cheras

Appendix C - Gold award in 27th International Invention, Innovation &
Tehcnology Exhibition 2016

Appendix D - 3rd Place (IPTA/S) Inclusive Innovation Challenge Competition
2017 (Middle Zone)

LIST OF TABLES

	Page
Table 2.1 The composition of RH: Elemental and organic constituents of RH	19
Table 2.2 Amino acid constituents in the eccrine sweat	53
Table 3.1 Trials 1-75 with varied neutralisation conditions	82
Table 3.2 Trial 1-15 of varying emulsion constituents	83
Table 3.3 Summary of nature of precipitate formed with different parameters	95
Table 3.4 Size of SiNP produced from Trials 1 to 15	103
Table 3.5 IR spectroscopy absorptions by frequency regions for RH intermediates	115
Table 3.6 Yield percentage of SiNP _{sp} from RH	122
Table 3.7 Yield percentage of SiNP _{me} from RH	127
Table 4.1 Powder efficiency comparison tests	135
Table 4.2 Fingerprint quality assessment grades	138
Table 4.3 Findings of Wilcoxon Signed Rank test for scores of finger-marks retrieved from multiple donors, depletion and ageing studies upon each tested surface	166
Table 4.4 Findings of Wilcoxon Signed Rank test for scores of fingerprints retrieved from ageing studies of NPR and SPR upon each tested surface	176
Table 6.1 Powder efficiency comparison tests	220
Table 6.2 Yield percentages of CNP ₁₈ powder from RH	232

Table 6.3	Findings of Wilcoxon Signed Rank test for scores of fingermarks retrieved from multiple donors, depletion and ageing studies upon each tested surface	255
-----------	-------------------------------------------------------------------------------------------------------------------------------------------------------------	-----

LIST OF FIGURES

	Page
Figure 1.1 Outline of the scope of research	9
Figure 2.1 The 3D projections of the ridges from the surface of the skin	48
Figure 2.2 Ridge characteristics or minutiae	49
Figure 2.3 Pore distribution visible along the ridges of the fingerprint viewed under a stereomicroscope	49
Figure 3.1 The methodology of SiNP synthesis from RH	79
Figure 3.2 RHA precursors a) RH b) post-acid treated RH c) charred RH after acid treatment d) RHA	81
Figure 3.3 SS_{rh} solution a) concentrated b) restored to the original volume	89
Figure 3.4 SS_{rh} solution before and after precipitation a) aged SS_{rh} solution b) gel-like silica c) colloidal silica	91
Figure 3.5 Production of SiNP powder a) powder precipitate b) gel precipitate c) pellet frozen at -20 °C before drying d) freeze-drying of SiNP pellet	92
Figure 3.6 Silica gel after neutralisation without solvent addition a) sulphuric acid 6 M b) acetic acid 10 M	93
Figure 3.7 SEM images: SiNP precipitated without solvent a) 6 M sulphuric acid b) acetic acid 10 M	93

Figure 3.8	SEM images of SiNP precipitated using 5 M acetic acid and 5g/L SS _{rh} with different volumes of acetone a) 10 mL acetone b) 20 mL acetone c) 30 mL acetone d) 40 mL acetone	96
Figure 3.9	SEM images of SiNP precipitated using 5 M acetic acid and 5g/L SS _{rh} with different volumes of ethanol a) 10 mL ethanol b) 20 mL ethanol c) 30 mL ethanol	97
Figure 3.10	SEM images of SiNP precipitated using 5 M acetic acid and 5g/L SS _{rh} with different volumes of acetone addition a) 30 mL acetone b) 40 mL acetone	98
Figure 3.11	SiNP powder produced using different acids and 40 mL acetone to precipitate a) glacial acetic acid b) 10 M acetic acid c) 5 M acetic acid	100
Figure 3.12	SEM images: SiNP precipitated with solvent (40 mL acetone) a) glacial acetic acid b) 10 M acetic acid c) 5 M acetic acid	101
Figure 3.13	SiNP _{sp} powder	102
Figure 3.14	SEM images (50 000x): SiNP synthesised via microemulsion route trials 1 to 15	104
Figure 3.15	SiNP _{me} powder	106
Figure 3.16	Characterisation studies of RH original state; SEM images of RH a) inner surface b) outer surface c) cross section d) Stereomicroscope image of RH's outer surface e) EDS spectrum f) XRD spectrum	108

Figure 3.17	Characterisation studies of treated RH; SEM images a) cross-section b) outer surface c) silica on outer surface d) EDS spectrum e) XRD spectrum	110
Figure 3.18	Bar graph representing ICPMS results: The chart shows the trace metal impurities present in the RH sample before and after acid treatment	111
Figure 3.19	Characterisation studies of RHA a) SEM images of RHA a) outer surface b) inner surface c-d) SiNP in RHA e) EDS spectrum f) XRD spectrum	112
Figure 3.20	FTIR spectra a) untreated RH b) acid treated RH c) acid and heat treated RH d) RHA	114
Figure 3.21	Characterisations of SiNP _{sp} a-d) SEM micrographs e) EDS spectrum	116
Figure 3.22	Particle size distribution chart based on the size of particles measured from SEM micrographs of SiNP _{sp}	117
Figure 3.23	Characterisations of SiNP _{sp} a-b) TEM micrographs c) XRD spectrum d) FTIR spectrum	118
Figure 3.24	Characterisations of SiNP _{sp} a) Nitrogen adsorption/desorption isotherms at 77 K b) pore size distribution calculated from the adsorption branch of the isotherm using BJH method	120
Figure 3.25	Six different type of adsorption isotherm	122
Figure 3.26	Characterisation studies of SiNP _{me} a-d) SEM micrographs e) EDS spectrum	124

Figure 3.27	Particle size distribution chart based on the size of particles measured from SEM micrographs of SiNP _{me}	125
Figure 3.28	Characterisation studies of SiNP _{me} a-b) TEM micrographs c) XRD spectrum d) FTIR spectrum	126
Figure 3.29	Characterisations of SiNP _{me} a) Nitrogen adsorption/desorption isotherm at 77 K b) pore size distribution calculated from the adsorption branch of the isotherm using BJH method	128
Figure 4.1	Surfaces tested for SiNP _{sp} powder a) tiles b) glass c) APVC d) metal e) soda bottle f) glossy black card g) electrical tape h) keyboard i) steering wheel cover (leather) j) painted glossy wood	134
Figure 4.2	SEM images: Fingerprint develop with SiNP _{sp}	139
Figure 4.3	SEM images: Fingerprint developed using SiNP _{me}	140
Figure 4.4	SEM image (80 000x): SiNP _{me} smaller than 100 nm distributed along the ridges of the fingerprint	140
Figure 4.5	SiNP _{sp} powder viewed under white light	141
Figure 4.6	SiNP _{sp} powder viewed under alternate light sources and various filters	141
Figure 4.7	Fingermarks developed using SiNP _{sp} viewed under a) white light b) blue light and c) blue-green light	142
Figure 4.8	Latent fingerprints of natural, eccrine and sebaceous origin from three volunteers: upper halves developed using SiNP _{sp} and lower halves developed using WP	143

Figure 4.9	Fingermarks developed on black glass; Row A using SiNP _{sp} powder and Row B using WP	144
Figure 4.10	SEM images of a) SiNP _{sp} and b) WP	145
Figure 4.11	SEM images of developed fingermark; a-b) SiNP _{sp} powder and c-d) WP using natural fingermark on a glass surface	147
Figure 4.12	Fingermarks developed with SiNP _{sp} powder from 36 varied subjects of different ages, sexes, and races	149
Figure 4.13	Fingermarks developed with WP from 36 varied subjects of different ages, sexes, and races	150
Figure 4.14	Bar chart that reflects number of fingermarks in each score category obtained from multiple donor studies (refer to Table 4.2 for score categories)	151
Figure 4.15	Depletion study on APVC surface	152
Figure 4.16	Depletion study on tiles surface	152
Figure 4.17	Depletion study on glass surface	153
Figure 4.18	Depletion study on metal surface	153
Figure 4.19	Depletion study on painted wood surface	154
Figure 4.20	Depletion study on soda bottle surface	154
Figure 4.21	Depletion study on black electrical tape surface	155
Figure 4.22	Depletion study on glossy black card surface	155
Figure 4.23	Depletion study on glossy steering wheel cover surface	156
Figure 4.24	Depletion study on computer keyboard surface	156

Figure 4.25	Fingerprint scores developed using SiNP _{sp} and WP in the depletion studies on non-porous surfaces represented by line graphs	157
Figure 4.26	Fingerprint scores developed using SiNP _{sp} and WP in the depletion studies on semi-porous surfaces represented by line graphs	158
Figure 4.27	Fresh fingerprints developed on various surfaces using SiNP _{sp} and WP	159
Figure 4.28	Fingerprints developed on various surfaces using SiNP _{sp} powder after ageing at 50°C for one, two and three hours	160
Figure 4.29	Fingerprints developed on various surfaces using commercial WP after ageing at 50°C for one, two and three hours	161
Figure 4.30	Fingerprints developed on various surfaces using SiNP _{sp} powder after ageing at 100°C for one, two and three hours	162
Figure 4.31	Fingerprints developed on various surfaces using commercial WP after ageing at 100°C for one, two and three hours	163
Figure 4.32	Line charts represent fingerprint scores developed using SiNP _{sp} and WP in the accelerated ageing studies on non-porous surfaces	164

Figure 4.33	Line charts represent fingerprint scores developed using SiNP _{sp} and WP in the accelerated ageing studies on semi-porous surfaces	165
Figure 4.34	SiNP _{sp} a) powder b) NPR	168
Figure 4.35	Fingermarks developed after 1 hour using NPR and SPR	170
Figure 4.36	Fingermarks developed after 24 hours using NPR and SPR	171
Figure 4.37	Fingermarks developed after 48 hours using NPR and SPR	172
Figure 4.38	Fingermarks developed after 96 hours using NPR and SPR	173
Figure 4.39	Fingermarks developed after 144 hours using NPR and SPR	174
Figure 4.40	Line charts represent fingerprint grades at every ageing interval on all six surfaces	175
Figure 4.41	Fingermarks developed on electrical black tape after one-hour of submersion in stagnant tap water a) NPR b) SPR	177
Figure 4.42	Fingermarks developed using NPR viewed under alternate light sources without any filter a) blue-green light (445-510 nm) b) violet light (400 -430 nm)	177
Figure 4.43	Fingermarks developed with a) freshly prepared NPR b) NPR reagent stored for one year	178

Figure 5.1	Curcumin extraction a) turmeric b) dried turmeric immersed in ethanol c) filtration of solid particles	187
Figure 5.2	Carotenoids extraction a) dried red chillies b) digested in NaOH c) filtered and washed d) immersed in ethanol e) mixture filtered	188
Figure 5.3	Anthocyanin blue extraction a) butterfly pea flower b) flower immersed in ethanol c) mixture filtered	188
Figure 5.4	Anthocyanin purple extraction a) purple cabbage b) immersed in DO water c) filtration of residues	189
Figure 5.5	Spirulina tablets	189
Figure 5.6	Food dyes a) Ponceau 4R red b) FCF Brilliant Blue	190
Figure 5.7	Preparation of dyed SiNP powder a) mixture of SiNP and cornstarch b) mixture of powders containing dye and ethanol	192
Figure 5.8	Dyed SiNP dried in an oven	192
Figure 5.9	Forensic light source (Crime-Lite® 2)	193
Figure 5.10	Surfaces used for coloured powder testing a) plastic beg b) plastic bottle c) shiny cardboard box d) wallpaper e) leather purse f) fluorescent sticker g) porcelain glass h) metal tin i) metal can j) measuring cylinder	193
Figure 5.11	Concentrated extracts of natural dyes a) curcumin b) anthocyanin purple c) anthocyanin blue d) carotenoid e) phycocyanin	194

Figure 5.12	Synthetic dyes a) Ponceau 4R food dye b) Brilliant Blue FCF c) crystal violet d) safranin	194
Figure 5.13	UV Vis spectra of natural dyes a) curcumin (426 nm) b) anthocyanin purple (551 nm) c) anthocyanin blue (617, 572 nm) d) carotenoids (438 nm) e) phycocyanin (628 nm)	195
Figure 5.14	UV Vis spectra of synthetic dyes a) Ponceau 4R food dye (506 nm) b) Brilliant Blue FCF (622 nm) c) crystal violet (579 nm) d) safranin (513 nm)	196
Figure 5.15	Natural dyes viewed under white light (top row) and UV light (bottom row)	196
Figure 5.16	Synthetic dyes viewed under white light (top row) and UV light (bottom row)	197
Figure 5.17	Natural dyed SiNP powders a) fresh b) after one year	198
Figure 5.18	Synthetic dyed SiNP powders a) fresh b) after one year	198
Figure 5.19	Dyed SiNP powders containing corn starch a) 10% corn starch b) 20% corn starch c) 30% corn starch d) 40% cornstarch	199
Figure 5.20	Fingermarks developed using dyed SiNP powders a) 10% corn starch b) 20% corn starch c) 30% corn starch d) 40% cornstarch	199
Figure 5.21	Multicoloured SiNP powders	199
Figure 5.22	FESEM micrographs of multicoloured SiNP powders	200

Figure 5.23	FTIR spectra of naturally dyed SiNP a) phycocyanin b) curcumin	201
Figure 5.24	FTIR spectra of synthetically dyed SiNP a) Brilliant blue FCF b) crystal violet c) safranin O d) Ponceau 4R	202
Figure 5.25	Fingermarks developed with coloured SiNP powders viewed under UV light (350-380 nm)	203
Figure 5.26	Fingermarks developed using coloured SiNP powders and viewed under blue-green light (445 - 510 nm)	204
Figure 5.27	Fingermarks developed using coloured SiNP powders and viewed under blue light (420 – 470 nm)	204
Figure 5.28	Photoluminescence of fingermarks developed using pink SiNP powder	204
Figure 5.29	Photoluminescence of fingermarks developed using red SiNP powder	205
Figure 5.30	Photoluminescence of fingermarks developed using yellow SiNP powder	205
Figure 5.31	Pink, red and yellow SiNP powders viewed under different light sources	205
Figure 5.32	Developed fingermarks on a non-porous plastic surface viewed under blue-green light with an orange filter	206

Figure 5.33	Developed fingerprints on a non-porous metal surface viewed under blue-green light with an orange filter	207
Figure 5.34	Developed fingerprints on a non-porous metal surface viewed under blue-green light with an orange filter	207
Figure 5.35	Developed fingerprints on a non-porous glass surface viewed under blue-green light with an orange filter	207
Figure 5.36	Developed fingerprints on non-porous porcelain surface viewed under blue-green light with an orange filter	207
Figure 5.37	Developed fingerprints on a semi-porous plastic surface viewed under blue-green light with an orange filter	208
Figure 5.38	Developed fingerprints on a semi-porous shiny cardboard surface viewed under blue-green light with an orange filter	208
Figure 5.39	Developed fingerprints on a semi-porous wallpaper surface viewed under blue-green light with an orange filter	208
Figure 5.40	Developed fingerprints on a semi-porous corrugated leather surface viewed under blue-green light with an orange filter	208

Figure 5.41	Developed fingerprints on a semi-porous fluorescent sticker surface viewed under blue-green light with an orange filter	209
Figure 5.42	SEM micrographs of luminescent powder particles a-b) commercial yellow luminescent powder c-d) SiNP	209
Figure 6.1	Acid treatment of RH	215
Figure 6.2	Alkali treatment of acid-treated RH	215
Figure 6.3	Purification of carbon a) removal of silica b) drying of the filtrate	216
Figure 6.4	CNP preparation a) acid treatment b) filtration c) ageing of filtrate in oven d) aged colloidal solution in eppendorf tubes e) centrifugation at 5000 rpm for 15 minutes	217
Figure 6.5	Surfaces used for CNP testing a) CD-ROM b) phone screen protector c) painted glossy wood d) stainless steel tool e) porcelain crucible f) credit card g) PVC electrical switch h) brown tape i) currency note j) translucent plastic	219
Figure 6.6	RH a) after heat treatment b) after the heat and acid treatment	221
Figure 6.7	SEM micrographs of acid-digested RH at different magnifications (a-d): EDS analysis of the bright white spots revealed the presence of silica	222

Figure 6.8	Carbon purification a) extracted silica b) carbon powder	222
Figure 6.9	SEM micrograph of carbon powder synthesised through a top-down approach	223
Figure 6.10	CNP intermediates a) filtrate from RH acid treatment b) aged filtrate c) CNP precipitate d) dried CNP liquid in crucible e) CNP powder	223
Figure 6.11	CNP produced from different ageing periods a) CNP ₁₂ b) CNP ₁₅ c) CNP ₁₈ d) CNP ₄₈	224
Figure 6.12	Fingermarks developed with a) CNP ₁₂ b) CNP ₁₅ c) CNP ₁₈ d) CNP ₄₈	224
Figure 6.13	Particle size distribution chart based on the size of particles measured from SEM micrographs of CNP	227
Figure 6.14	Characterisations of CNP a-d) SEM images of CNP e) EDS spectrum f) FTIR spectrum	228
Figure 6.15	Characterisations of CNP a-d) TEM images of CNP e) XRD spectrum	229
Figure 6.16	Digital photographs of fluorescent CNPs a) under white light b) under UV lamp (365 nm)	230
Figure 6.17	Characterisations of CNP ₁₈ a) Nitrogen adsorption/desorption isotherms at 77 K b) pore size distribution calculated from the adsorption branch of the isotherm using BJH method	231

Figure 6.18	Latent fingerprints of natural, eccrine and sebaceous secretion from three volunteers; upper halves developed using CNP ₁₈ and lower halves developed using BP	233
Figure 6.19	Fingerprints developed on porcelain crucible; Row A using CNP ₁₈ powder and Row B using BP	234
Figure 6.20	SEM images: Fingerprints developed with CNP ₁₈	234
Figure 6.21	SEM images of a) CNP ₁₈ and b) BP	235
Figure 6.22	SEM images of developed fingerprints; a-b) CNP ₁₈ powder and c-d) BP using natural fingerprint on a glass surface viewed at different magnifications	236
Figure 6.23	Fingerprints developed using CNP ₁₈ (upper halves) and BP (lower halves) from 36 volunteers of various age, sex and race	238
Figure 6.24	Bar chart that reflects the number of fingerprints in each score category obtained from multiple donor studies (refer to Table 4.2 for score categories)	239
Figure 6.25	Depletion study on CD-ROM	240
Figure 6.26	Depletion study on tempered glass	241
Figure 6.27	Depletion study on glossed wood	241
Figure 6.28	Depletion study on a stainless steel tool	242
Figure 6.29	Depletion study on porcelain crucible	242
Figure 6.30	Depletion study on electric switches (Bakelite polymer)	243

Figure 6.31	Depletion study on credit card (polyvinyl chloride acetate)	243
Figure 6.32	Depletion study on brown tape (polypropylene)	244
Figure 6.33	Depletion study on paper money (polypropylene)	244
Figure 6.34	Depletion study on white translucent plastic	245
Figure 6.35	Fingerprint scores developed using CNP ₁₈ and BP in the depletion studies on semi-porous surfaces represented by line graphs	245
Figure 6.36	Fingerprint scores developed using CNP ₁₈ and BP in the depletion studies on non-porous surfaces represented by line graphs	246
Figure 6.37	Fresh fingerprints developed on various surfaces using CNP ₁₈ and BP	247
Figure 6.38	Fingerprints developed on various surfaces using CNP ₁₈ powder after aged at 50°C for one, two and three hours	249
Figure 6.39	Fingerprints developed on various surfaces using BP after aged at 50°C for one, two and three hours	250
Figure 6.40	Fingerprints developed on various surfaces using CNP ₁₈ powder after aged at 100°C for one, two and three hours	251
Figure 6.41	Fingerprints developed on various surfaces using BP after aged at 100°C for one, two and three hours	252

Figure 6.42	Fingermark scores developed using CNP ₁₈ and BP in the accelerated ageing studies on nonporous surfaces represented by line graphs	253
Figure 6.43	Fingermark scores developed using CNP ₁₈ and BP in the accelerated ageing studies on semi-porous surfaces represented by line graphs	254
Figure 6.44	Multicoloured SiNP powders	260
Figure 6.45	ECO ^{fp} fingerprint kit consisted of white SiNP powder, black CNP powder, multicoloured SiNP powder and NPR	260

LIST OF ABBREVIATIONS

APVC	-	Acrylic polyvinyl chloride
BET	-	Brunauer- Emmett-Teller
BJH	-	Barrett–Joyner–Halenda
BP	-	Black powder
CNP	-	Carbon nanoparticle
DFO	-	1,8-Diazafluoren-9-one
DNA	-	Deoxyribonucleic acid
EDS	-	Energy Dispersive X-Ray Spectrophotometer
FESEM	-	Field Emission Scanning Electron Microscope
FTIR	-	Fourier Transform Infrared Spectrophotometer
GNP	-	Gold nanoparticle
HCl	-	Hydrochloric acid
HRTEM	-	High Resolution Transmission Electron Microscope
ICPMS	-	Inductively Coupled Plasma Mass Spectrophotometer
IR	-	Infrared
KBr	-	Potassium bromide
MMD	-	Multimetal Deposition
NaOH	-	Sodium hydroxide

NPR	-	Nanoparticle Reagent
QD	-	Quantum dots
RH	-	Rice husk
RHA	-	Rice husk ash
SEM	-	Scanning Electron Microscopy
SiNP	-	Silica nanoparticle
SiNP _{sp}	-	Silica nanoparticle _{solvent precipitation}
SiNP _{me}	-	Silica nanoparticle _{microemulsion}
SMD	-	Single Metal Deposition
SPR	-	Small Particle Reagent
SS	-	Sodium silicate
SS _{rh}	-	Sodium silicate _{rice husk}
TEM	-	Transmission electron microscopy
TEOS	-	Tetraethyl orthosilicate
UV	-	Ultraviolet
UV-Vis	-	Ultraviolet-Visible
WP	-	White powder
XPS	-	X-Ray Photoelectron Spectrophotometer
XRD	-	X-Ray Diffraction analysis

SINTESIS NANOPARTIKEL SILIKA DAN KARBON DARIPADA SEKAM PADI UNTUK APLIKASI CAP JARI PENDAM

ABSTRAK

Mutakhir ini, penyelidikan yang melibatkan teknik penimbunan cap jari pendam (CJP) telah mengambil pelbagai laluan dalam usaha para penyelidik meneroka kaedah alternatif untuk meningkatkan keberkesanan serbuk dan reagen yang sedia ada. Pelbagai kajian tentang kesan penggunaan sebatian nano untuk meningkatkan sensitiviti dan selektiviti serbuk cap jari yang boleh menimbulkan CJP dengan kejelasan dan kontras yang tinggi aktif dijalankan. Namun, aplikasi nanoteknologi dalam penyiasatan rutin adalah terhad disebabkan oleh kekangan kos, syarat aplikasi yang ketat dan juga sifat toksik nanopartikel sintetik. Dalam kajian ini, kaedah sintesis yang baru telah dibangunkan untuk sintesis nanopartikel silika (NS) dan karbon dengan menggunakan sumber mesra alam, sekam padi (SP). Proses pencernaan asid telah dijalankan untuk menyingkirkan sisa kotoran logam dari SP. Sisa penapisan telah diabukan untuk mengestrak silika, manakala baki cecair pula dipanaskan untuk membentuk nanopartikel karbon (NK), teknik sintesis NK yang baru. Natrium silikat telah dijana dengan melarutkan abu SP tulen yang diperolehi dari proses penulenan berperingkat, dalam solusi alkali. Pemendakan NS yang berbentuk sfera, tidak beraglomerasi dan mempunyai purata saiz partikel 270 nm dengan menggunakan asid asetik dan aseton juga diterajui dalam kajian ini. Komposisi kimia dan ciri amorfos silika telah ditentukan dengan menggunakan teknik analisa spektroskopi. Pengeringan beku menghasilkan serbuk NS yang mempunyai isipadu liang mesoporos ($0.167 \text{ cm}^3/\text{g}$), purata saiz liang 4.2 nm (0.9 hingga 57.90 nm distribusi saiz liang) dan jumlah luas permukaan yang tinggi ($162.00 \text{ m}^2/\text{g}$ (Brunauer-Emmett Teller), (BET) dan

238.60 m²/g Barrett-Joyner-Halenda (BJH)). Proses penuaan sisa cecair dari pencernaan asid SP pula telah menghasilkan NK yang mempamerkan ciri-ciri partikel yang berbentuk sfera, berpermukaan kasar dengan tahap aglomerasi yang lebih tinggi berbanding NS. Distribusi saiz partikel NK adalah dalam linkungan 100 hingga 500 nm dengan saiz partikel purata 300 nm. Ikatan molekul dan komposisi kimia NK telah disahkan dengan menggunakan teknik-teknik spektroskopi. Serbuk NK mempunyai isipadu liang mikroporos (0.009 cm³/g), saiz liang purata 61.75 nm (0.89 hingga 81.90 nm distribusi saiz liang) dan jumlah luas permukaan yang rendah (0.558 m²/g BET dan 4.816 m²/g BJH). NS yang dibentuk telah digunakan dalam tiga produk berbeza; serbuk nanopartikel putih, reagen nanopartikel serta serbuk nanopartikel pelbagai warna, manakala NK digunakan sebagai serbuk nanopartikel hitam. Pendekatan metodologikal telah diambil untuk membandingkan keberkesanan serbuk nanopartikel dengan serbuk cap jari komersial untuk penimbunan CJP pada peringkat penuaan yang berbeza. Sistem skor standard telah digunakan untuk menilai keputusan dan analisa statistik digunakan untuk mendapatkan kesimpulan data. Dapatan kajian menunjukkan bahawa keberkesanan serbuk nanopartikel adalah setanding dan adakalanya lebih baik dari serbuk komersial pada permukaan yang tertentu. Sintesis nanopartikel ini menggunakan bahan mentah yang murah tidak memerlukan alatan khas, penambahan resin, molekul pelekat atau proses pasifasi permukaan. Selain itu, penggunaan SP dapat meningkatkan sumber kewangan para petani dan juga mengabungkan kaedah nanoteknologi yang mesra alam dalam siasatan kriminal rutin. Secara konklusi, produk-produk murah yang telah dicadangkan mempamerkan kualiti lebih unggul dan superior berbanding dengan produk dalam pasaran kini.

SYNTHESIS OF SILICA AND CARBON NANOPARTICLES FROM RICE HUSKS FOR LATENT FINGERMARKS APPLICATION

ABSTRACT

Research into latent fingerprint developing techniques has taken many paths over the years as researchers and practitioners explore numerous methods to enhance existing powders and reagents. Currently, copious research is being dedicated to investigating the transformational improvements that could be provided by nanosized compounds to expand the sensitivity and selectivity of fingerprint dusting powders to develop fingerprints with high clarity and better contrast. Nonetheless, such a technique has inherent drawbacks of limited field applicability, cost and energy intensive, incurs health hazard to the users in the long run as well as prepared using synthetic precursors. In this research novel synthesis techniques of silica nanoparticle (SiNP) and carbon nanoparticle (CNP) from a sustainable eco-friendly source, rice husk (RH) was developed. Acid digestion process was conducted to remove trace metal impurities from RH. The filtrand was ashed to extract silica, while the filtrate was aged to form CNP, a novel CNP synthesis technique pioneered in this research. Sodium silicate was formed by dissolving highly pure rice husk ash, obtained from the stepwise purification of RH, in alkali solution. Precipitation of SiNP using acetic acid and acetone is introduced in this research to form minimally agglomerated, well dispersed spherical SiNP with a mean particle size of 270 nm, verified using imaging techniques. Silica chemical composition and amorphous nature were confirmed by using spectroscopic analysis. Freeze-drying produced mesoporous pore volume (0.167 cm³/g) silica powders with a 4.2 nm average pore size (0.9 to 57.9 nm pore size

distribution) and very high specific surface ($162.00 \text{ m}^2/\text{g}$ (Brunauer-Emmett Teller, (BET) and $238.60 \text{ m}^2/\text{g}$ Barrett-Joyner-Halenda (BJH)). Ageing of the filtrate from acid digestion produced amorphous CNP that exhibited non-smooth, slightly irregular spherical particles with a higher degree of agglomeration in comparison to SiNP. Particle size distribution fell in the range of 100 to 500 nm with mean particle size of 300 nm. Molecular bonding and chemical composition of the CNP was confirmed using spectroscopic techniques. CNP powder possessed microporous pore volume ($0.009 \text{ cm}^3/\text{g}$) with a 61.75 nm average pore size (0.89 to 81.90 nm pore size distribution) and low surface area value ($0.558 \text{ m}^2/\text{g}$ BET and $4.816 \text{ m}^2/\text{g}$ BJH). Spherical SiNP obtained was formulated into three derivative products namely white nanoparticle powder, nanoparticle reagent (NPR) and multicoloured nanoparticle powder, while the CNP powder was used as the black nanoparticle powder. A methodological approach was conducted to compare the efficiency of the nanoparticle products against commercial products by developing fresh and aged fingerprints of various stages. Standard scoring system was applied to evaluate the results and statistical analysis was employed to summarise the data. Findings revealed that the nanoparticle powders and reagent performed on par with the existing commercial powders while exhibiting higher selectivity. Nanoparticle synthesis from low cost precursor in this research did not require special equipment, addition of resins/adhesives or surface passivation. Additionally, utilisation of RH may boost farmer's income and incorporate non-toxic green nanotechnology into routine investigative procedures. In conclusion, the low cost products developed exhibited promising quality and superiority to the existing products in the market.

CHAPTER 1

INTRODUCTION

1.1 Research background

Fingermarks are the most affirmative biometric evidence. There are continuous efforts to broaden new techniques and improving current techniques of fingermark development with enhanced sensitivity (Becue *et al.*, 2007). The improved technique is aimed to produce fingermarks with better clarity and resolution at various stages of ageing regardless of surface porosity. Increasingly more innovative strategies are advanced targeting precise components of fingermark residue simultaneously improving the sensitivity of the technique and enhancing contrast (Drapel *et al.*, 2009). In this line, luminescent fingermark visualisation offers remarkable advantages on a wider variety of light, dark and patterned surfaces providing enhanced contrast (Sodhi and Kaur, 2008).

Nanotechnology is a fascinating branch of science. Physicochemical properties of nanomaterial tuneable by size modulation offer uncountable opportunities for surprising discoveries (Heiligtag and Niederberger, 2013). Incorporation of nanotechnology in diverse fields has brought fundamental improvement including the sector of forensic science specifically in latent fingermark development techniques (Zaman *et al.*, 2014). Nanoparticles can be exploited in designing new fingermark dusting powders and reagents with expanded selectivity and sensitivity (Dilag *et al.*, 2011).

Nanoparticles are small in size, versatile and their surface properties may be tuned according to the needs which lead to the precise targeting of a specific component of

fingermark residue apart from the underlying substrate (Moret *et al.*, 2014). However, the commercialisation of those new techniques is often limited due to employment conditions, the limited mobility of the substrate bearing fingermark or the increased health hazard to the consumer (Becue *et al.*, 2011). An ideal and improved product should no longer offer only enhanced selectivity and sensitivity but also may be employed for regular use without or with minimal health threat to consumers (Becue *et al.*, 2007).

1.2 Fingermarks and forensic investigations

The use of ridge impressions has been recorded as early as 221 B.C in a Chinese document and since then the evidentiary evolution of fingermarks has only solidified its undisputed value (Voss-De Haan, 2006). Fingermarks are surely one of the most crucial and incriminating proof in the course of a criminal investigation. Lower processing fee and concrete fundamental science behind dactylography make fingermark evidence very valuable to crime scene professionals (Barnes, 2011). Fingermark does not best serve to link the crime scene to a suspect alone but may also be used as a mean of victim identification and exoneration of the innocent.

The first case known to man to have secured a conviction primarily based on fingerprint evidence took place in Bengal in 1898 (Sodhi and Kaur, 2005). Alphonse Bertillon solved a murder in France, Paris via matching a fingermark found at a crime scene with his anthropometric cards (SIRCHIE, 2011). This incident instigated the cascade of cases using fingerprints as a treasured tool for identification in forensic science. Studies have been carried out to continue improving method of detection, recovery and identification of fingermark.

Most of the time, fingerprints require development to permit the visualisation. Abundant physical and chemical techniques are currently dedicated for this purpose. All of the techniques have inherent limitations in their application or efficiency. Factors such as nature of substrate bearing the fingerprint, conditions of fingerprint recovery, and the composition of the fingerprint residue and age of the recovered fingerprint play a major role in influencing the capability of a technique.

1.3 Problem statement

The detection, comparison and identification of fingerprints remain the best means of providing links between the trifecta of crime; the victim, crime scene and the perpetrator. Significant ongoing research is being directed to improve the sensitivity of the existing latent fingerprint development methods owing to the fact that current techniques may not be effective on weak fingerprints or reveal sufficient ridge details for identification (Lennard, 2014). In spite of the paramount value of fingerprints as an identification tool, the recovery rate of latent fingerprints found in crime scenes is not at a satiable level. Loss of fingerprints may be attributed to the destructive environment such as human act, arson, explosion, rain and natural conditions of ageing (Dhall and Kapoor, 2016). Fingerprint developing products that are currently in commercial use poses several disadvantages including high cost, increased health hazard, non-specific interaction with ridge residue and background, requires the use of one brush for each powder as well as environmental contamination (Lee and Gaensslen, 2012; Daluz, 2015).

The effectiveness of fingerprint development heavily relies on the size and shape of the fingerprint powder particles. Optimal fingerprint developing products would have the following attributes; small, rounded and well-dispersed particles, which has a high

affinity for the fingerprint residue but exhibits minimal interaction with the substrate bearing the fingerprint (Sodhi and Kaur, 2001). Smaller and rounded particles have better adherence and create a uniform layer on the ridge than large coarse particles. Other added advantage of an optimal product would include increased stability, cost-effective, field-friendly, easy manufacturing from a sustainable source and poses a minimal health hazard for the users (Fernandes *et al.*, 2015). However, most commercial formulation still utilises fine nanostructured particles in the range of one to ten micrometres (Sodhi and Kaur, 2001). These particle does not have any specific affinity for fingerprint residue and this characteristic leads to non-specific interaction between fingerprint residue and the particles (Becue *et al.*, 2009).

Besides, commercial fingerprint dusting powders may cause great health hazard in the long term. Although a substantial amount of fingerprint powder may be inhaled by the crime scene professionals and police personnel during crime scene analysis, secondary exposure from contaminated clothing was deemed to be more harmful. Health hazard from the long-term exposure to fingerprint dusting powder is caused by the presence of trace metals that lead to heavy metal toxicity (Netten *et al.*, 1990; Maynard, 2011). Exposure to fingerprint dusting powders can cause skin rashes and visual impairment in the long run (Souter *et al.*, 1992).

Although nanoparticle-based techniques and powders have been extensively researched in the past and continuing efforts are being undertaken to optimise these techniques, production of fingerprint dusting powder with small, well dispersed and rounded particles have yet to be reported. Additionally, many of the varied powders introduced mainly use synthetic precursors, including titanium dioxide and silica powders (Becue *et al.*, 2007; Theaker *et al.*, 2008; Arshad *et al.*, 2015; Moret *et al.*,

2016). The preparation of precursors used for the commercial and previously proposed product synthesis consumes significant cost and energy. Enhancement of the sensitivity was proposed to be possible but at a higher cost than the current methods. Moreover, the techniques that have been proposed have limited field applicability and eliminate possible recovery of other evidence present on the substrate bearing the fingerprint (Sodhi and Kaur, 2017).

Techniques such as multimetal deposition (MMD) and vacuum metal deposition have limitations such as extremely narrow pH conditions for effective development, carcinogenic properties, costly and destructive in nature (Gao *et al.*, 2009). Functionalisation of nanoparticles may increase the precision of the particle interaction with a specific component of the residue (Leggett *et al.*, 2007), but obstacle arises when the presence of a targeted component is insufficient. The aqueous nature of the functionalised nanoparticles contaminates the surface and destroys the fingerprint residue. Contamination makes it unlikely for the retrieval of other forensic evidence such as drug detection or deoxyribonucleic acid (DNA) extraction. As a result, these techniques are often used as a last resort of attempt at fingerprint recovery.

The widespread interest in nanoparticles arises due to several inherent advantages as compared to conventional techniques on account of their small size that enables high-resolution fingerprint development. Besides, their quantum confinement property enables the production of luminescent prints as well as a wide range of surface modification potential that targets specific component (Moret *et al.*, 2016). Generally explored nanoparticles for fingerprint detection include gold and silver nanoparticles as well as metal oxides, such as titanium dioxide, aluminium oxide and zinc oxide (Stauffer *et al.*, 2007; Chadwick *et al.*, 2012; Sodhi and Kaur, 2017). However, most

nanoparticles has weak or no luminescence at all which confine their applications to light coloured surfaces to provide sufficient contrast.

Conferring luminescent property to these nanoparticles although possible, requires a tedious protocol and still limited to non-porous surfaces only. Use of quantum dots (QD) is also limited because surface functionalisation to improve selectivity comes at the expense of altering the structural and luminescence properties. Hence, despite the collective efforts of introducing nanoparticle-based fingerprint detection techniques, each technique lack either one of the following factors; small size, optical properties or surface modification.

One type of nanoparticles that possesses all the three factors combined in one entity is the silica nanoparticles (SiNPs). Nonetheless, application of SiNP for fingerprint development has not been strongly researched until recently. SiNPs consists of a porous matrix made up of siloxane bonds, with an outer layer of silanol bonds which are highly reactive with alkoxysilanes offering limitless functionalisation capacity. In addition, dye molecules can be easily entrapped into the porous matrix conferring photoluminescent properties to the SiNP. Copious synthesis methods exist for fabrication of SiNPs, but Stober's synthesis and reverse microemulsion techniques are the most generally employed techniques. Stober's synthesis offers bulk production meanwhile reverse microemulsion offers better control over the size and surface of the SiNP nevertheless with a lower yield. Additionally, these techniques exploit synthetic precursors such as tetraethyl orthosilicate (TEOS).

A few reports regarding the application of SiNP synthesised via these routes using expensive synthetic precursors for latent fingerprint development has been previously reported (Theaker *et al.*, 2008; Reip *et al.*, 2010; Moret *et al.*, 2016). In addition to

the higher cost and energy consumption for the production of the synthetic precursors utilised, these techniques produced highly agglomerated nanostructured SiNPs in powder form. The SiNP suspension upon drying was also reported to be crystalline in nature, translating into the fact that the particles possess lattice structure which is unsuitable for fingerprint development according to much previous literatures (Wilshire, 1996; Sodhi and Kaur, 2001).

Abundant research has been dedicated to extracting silica from rice husk (RH) in amorphous or crystalline form. Nevertheless, these research prioritised extraction of highly porous SiNP in the smallest size, regardless of the agglomeration state primarily to be applied as fillers, absorbents or drug carriers (Hassan *et al.*, 2014; Noushad *et al.*, 2014; Abu *et al.*, 2016). Prior to this research, silica extracted from RH has never been applied for the development of fingerprint, which require particles of different morphology such as small sized, spherical and minimally agglomerated.

The goal of this study was to address lack of fingerprint developing products that comprises of well-dispersed nanoparticles that have specific shape and size that simultaneously exhibit higher selectivity and sensitivity to fingerprint residue. Other than that, the nanoparticles were produced from agricultural waste, RH, which not only serve to recycle waste products but also to minimise manufacturing cost and health hazard to the users. Lowering the cost of the products will significantly improve the reach of the technology to all potential customers. Hence, enabling easy incorporation into routine forensic investigations.

1.4 Aim and objectives

The principal aim of this research was to fabricate nanoparticles from RH and to assess their use as potential latent fingerprint developing powders and reagent with increased selectivity and sensitivity.

Specific objectives of this research were:

- 1) To establish an optimised extraction procedure of pure SiNP and carbon nanoparticle (CNP) from rice husk ash (RHA) for production of nanoparticle powders ideal for the development of latent fingermark on dark or light non-porous and semi-porous surfaces and their characterisation using various imaging and analytical techniques.
- 2) To formulate nanoparticle reagent (NPR) using SiNP powder for the development of fingermark on wet and sticky surfaces.
- 3) To produce multicoloured SiNP powders with photoluminescence property using natural or synthetic dyes for the development of latent fingermark on multicoloured and patterned surfaces.
- 4) To investigate the effectiveness of the nanoparticle powders and reagent in comparison to commercial products on fresh and aged fingermarks in controlled laboratory settings as well as in field study with the Royal Malaysian Police.

1.5 Scope of research

This research was conducted in a few phases, which are outlined in **Figure 1.1**.

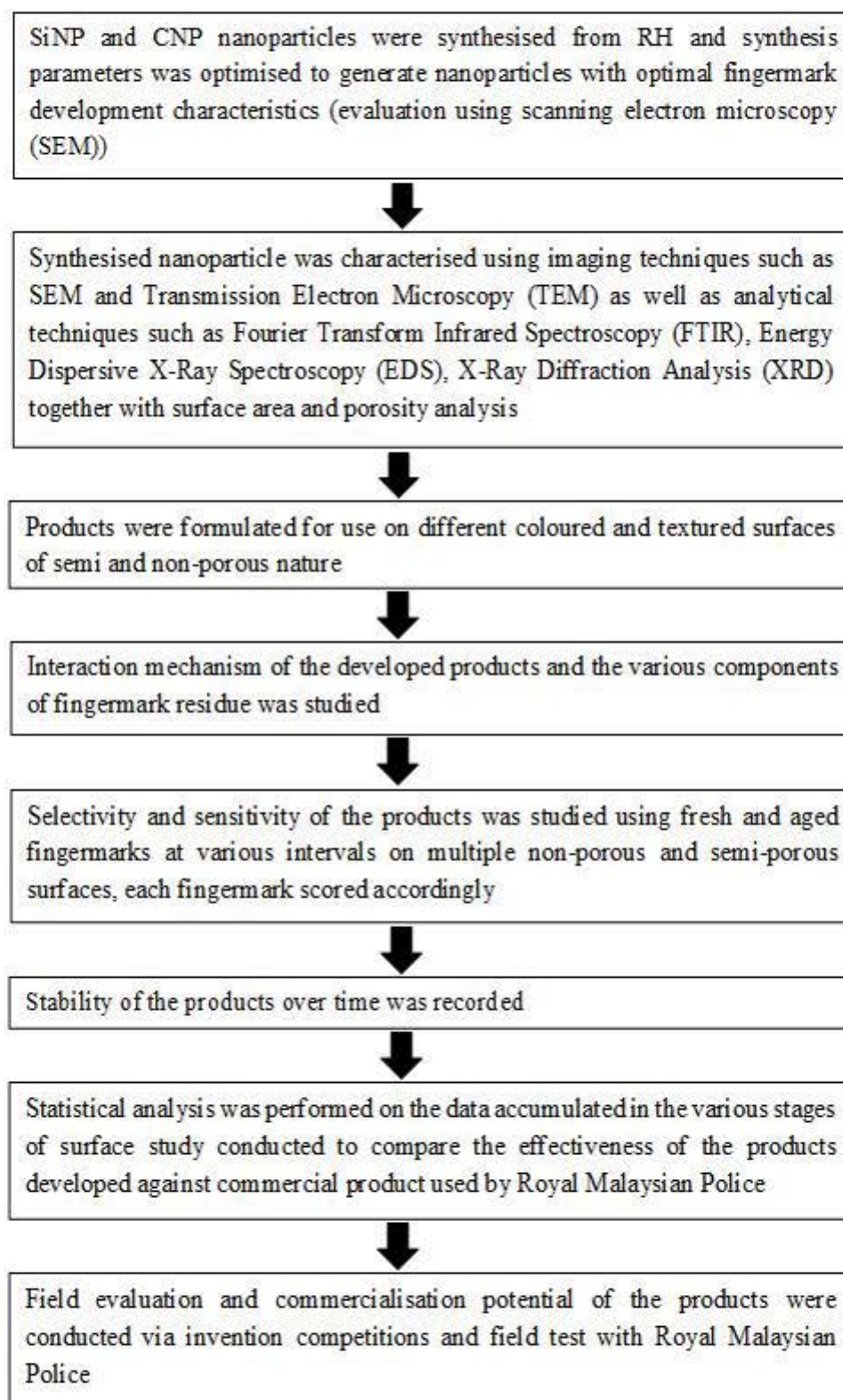


Fig. 1. Outline of the scope of research

1.6 Thesis outline

The first chapter elaborates the research background, problem statement, the gap of knowledge as well as the aims and objectives of this research. The second chapter of this thesis encompasses an elaborate definition of the terms used throughout this thesis and the literature review of the key components of this thesis. The third chapter encompasses the extraction of silica from RH and subsequent synthesis of SiNP with optimal characteristic for fingerprint development.

Chapter 4 illustrates the application of the synthesised SiNP powder as dry and wet powder suspension for the development of fingerprints on various non-porous and semi-porous surfaces, studying the interaction, selectivity, sensitivity of the powder and reagent. Chapter 5 describes the extraction of natural dye pigments and doping them into the SiNP powder in order to produce fluorescent SiNP powders that provide better contrast on multi-coloured surfaces.

Chapter six depicts the synthesis steps of spherical CNP from RH and the subsequent application along with the sensitivity and selectivity analysis on various non-porous and semi-porous surfaces. The fingerprint kit comprised of the white and multicoloured SiNP powder, black CNP powder and NPR (ECO^{fp} Fingerprint Kit) is introduced in this chapter as well. Chapter seven discusses the conclusions, limitations and future studies recommendations for this research.

CHAPTER 2

LITERATURE REVIEW

2.1 Nanoparticles

Nanoparticles research are a fascinating branch of science. A scientifically correct definition of nanoparticle has yet to be provided (Boverhof *et al.*, 2015). Most widely accepted definition of the nanoparticle is an individual entity having all three-dimensional measurement or at least one dimension measuring in the range of 1 to 100 nm (Moreno-Vega *et al.*, 2012). Although the range of 1 to 100 nm is used to define nanoparticles, there is no evidence supporting begin and abrupt ending of physical and chemical attributes of nanoparticles below and above this range. For example, many properties characteristic of nanoparticles still continues well above the upper limit of 100 nm (Lidén, 2011; Maynard, 2011).

Therefore, a more inclusive definition of nanoparticles has been proposed considering the fact that particle size distribution alone is not enough to provide an accurate definition. Authorities such as Taiwan Council of Labour Affairs and European Commission have set two conditions to be met for nanoparticle inclusion. The material either possesses one or more external dimension in the nanoscale range or beyond this range but exhibits nanoscale properties such as increased chemical reactivity (Health-Canada, 2011; Lidén, 2011; Taiwan, 2012).

Another report suggested the use of the following three categories to define different levels of nanomaterial. Category one is the nanomaterial with a mean particle size larger than 500 nm. In the category, the lower limit of size would most likely be above the designated 100 nm cut-off. Thus, further investigation regarding nanoscale properties is required for inclusion in nanoparticle range. Category two is where the

mean particle size lies between 500 nm and 100 nm, where it is more than likely that part of the size distribution will be lower than 100 nm. Hence, that material may be considered nanomaterial and more detailed characterisations are required to do the correct determination. The third category is when the mean particle size falls in between the range of 1 and 100 nm and are considered nanomaterial (Auvinen *et al.*, 2010).

Advantages of using nanoparticle for fingerprint development have been widely researched (Becue *et al.*, 2007; Moret *et al.*, 2014). SiNP in the range of 400 to 500 nm has been reported to develop fingerprint with sufficient clarity (Theaker *et al.*, 2008). Another study utilised nanostructured zinc oxide with a flower-like structure with aggregated dimensions measuring up to one micrometre for fingerprint development. The developed fingerprints exhibited clear ridge detail (Choi *et al.*, 2008a). Alternatively, dye-doped nanophosphors with the dimension 300 to 500 nm that were also investigated for fingerprint development reported positive outcome for extremely dry fingerprints (Reip *et al.*, 2010).

2.1.1 Nanoparticle synthesis

Synthesis of nanoparticles can be categorised into two most basic methods that are either the top-down or the bottom-up approaches. The precursor material used for these techniques can either be of synthetic or natural in origin (Noushad *et al.*, 2012; Moret *et al.*, 2014). The purity of the final product and particle size distribution are ultimately governed by the nature of the manufacturing process and any integral purification steps involved, such as acid digestion or calcination for silica extraction from RH (Vaibhav *et al.*, 2015). The top-down or the physical method of nanoparticle creation is the fine division of the bulk element into their respective nanosized counterpart (Balasooriya *et al.*, 2017).

The bottom-up approach is a more commonly adapted chemical route of nanoparticle synthesis. Nucleation of the specific atom and subsequent or simultaneous aggregation of the atoms forms nanoparticles of the required size (Merza *et al.*, 2012; Rahman and Padavettan, 2012; Polte, 2015). The basis of the wet chemical reduction is the formation of an aqueous solution containing the element of interest and reducing the ions into atoms using any reduction agents (Sharma *et al.*, 2009). Sometimes a catalyst or stabilising agents accompany the process to aid in the formation of specific shape and size distribution of such nanoparticles via electrostatic repulsion or steric stabilisation (Abid *et al.*, 2002). For example, SiNP can be synthesised by reducing SS_{rh} prepared from RH silica (Lee *et al.*, 2017).

There are a few methods to control the size and shape of the particles formed during synthesis mainly by governing the different aspects of the nucleation and growth of the particles. It was observed that the addition of different acids and solvents affected the properties of SiNP formed from SS_{rh} (Noushad *et al.*, 2012). The stoichiometric ratio of the synthesis process is very important to control the pH, amount of reactants available and the time taken for the reaction to fully complete directly affecting the particle size (Wang *et al.*, 2010b). Capping agents such as surfactants offer control over particle size by coating the generated particles to form an electrostatic barrier to avoid further growth and also simultaneously stabilising the particles from agglomerating (Jana *et al.*, 2001).

The time taken for the reaction to complete has an inverse effect on the size distribution of the particles. As the time taken for the reaction is increased the gap between the newly formed nucleus and the first formed nucleus is multiplied. As a result, the particle size distribution will be huge because by the end of the process the first formed nucleus will acquire large growth as time increases (Jimenez-Ruiz *et al.*, 2015).

Separation of the nucleation and growth process, for example, the Turkevich method of gold nanoparticle (GNP) synthesis, can afford full control of the particle size. The nucleation of gold atoms are conducted separately to produce particles of 20 nm size and then seeded into a growth media in a specific ratio to produce particles double the size of the seeded nucleus (Kimling *et al.*, 2006).

Control over the number of reactants can be achieved by creating an emulsion containing the aqueous solution of the element, otherwise known as micelles. Dispersing tiny droplets of the elemental aqueous solution in the emulsion will limit the provision of the reactants thus, effectively limiting the growth of the particles (Finnie *et al.*, 2007). Alteration to any of the factors of nucleation and growth can lead to uncontrolled growth as well as large particle formation (Schnetz and Margot, 2001). The same principle can be applied to control the formation and aggregation of SiNP from RH.

2.1.2 Nanomaterial characterisations

A newly synthesised nanomaterial may be characterised using analytical instruments to understand its intrinsic structure and properties (Murdock *et al.*, 2008). New nanomaterial may be characterised by its morphological, structural and optical features as well as particle size and surface area analysis (Lu and Hsieh, 2012). Morphological characterisations warrant great attention because of its influence on various properties of the nanomaterial. Microscopic techniques such as scanning electron microscopy (SEM), transmission electron microscopy (TEM), polarised optical microscopy and atomic force microscopy offers a remarkable pathway to gleam morphological information of the nanomaterial at an elemental level. SEM offers information on the

surface level of the particles while TEM provides information on the bulk material from very low to higher magnifications (Zhou *et al.*, 2007; Egerton, 2016).

Structural properties of a nanomaterial can be obtained using instruments such as X-Ray Diffractometer (XRD), Energy Dispersive X-Ray Spectrophotometer (EDS), Fourier Transform Infrared Spectrophotometer (FTIR), X-Ray Photoelectron Spectrophotometer (XPS), Brunauer-Emmett-Teller (BET) and particle size analysis. Each instrument provides different structural information. XRD reveals the crystallinity and phase, EDS; the elemental composition, FTIR: structural bonds and material signature and BET for the total surface area determination. XPS is a more sensitive way of determining the exact elemental ratio and bonding nature of the elements (Als-Nielsen and McMorow, 2001; Schneider, 2011; Eckert, 2012).

Optical techniques are aimed to determine the absorption, reflectance, luminescence and phosphorescence properties of a nanomaterial. Analytical instruments such as Ultraviolet-Visible (UV-Vis) and fluorescent spectrophotometers can provide this information (Khan *et al.*, 2017). This is imperative to determine the interactions of the nanomaterial with the electromagnetic energy so that they can be engineered to fit the purpose of use.

2.2 SiNP

Silicon is the second most abundant element on the Earth's crust and due to its strong bond with oxygen atoms, it rarely exists as a pure element (Bansal *et al.*, 2006; Meng-Hao *et al.*, 2012; Liu *et al.*, 2013). Silicon often exists as crystalline silica (silicon dioxides) or synthetic amorphous form (silicates). Silica, a polymer of silicic acid consists of base units of the tetrahedral form of interlinked SiO₄ (Jal *et al.*, 2004).

Crystalline silicon is widely used in metallurgy, silicone synthesis and also in the

semiconductor industry. On the other hand, amorphous silica have unique properties that makes them exploitable in the ceramics, rubber fillers, pharmaceuticals, dental materials, biomedical, absorbent, nanoelectronics, photonics, biotechnology, energy harvesting, composite fillers, thermal insulators and thixotropic agents (Kamath and Proctor, 1998; Liou, 2004; Choi *et al.*, 2008b; Becue *et al.*, 2011; Rafiee *et al.*, 2012; Liu *et al.*, 2013; Noushad *et al.*, 2014).

Manufacturing of pure silica is energy-intensive when conventional raw materials are utilised (Mittal, 1997; Kalapathy *et al.*, 2002). Most common SiNP precursors are silicon alkoxides or silicates which in turn are synthesised from raw material like sand through smelting method (Kalapathy *et al.*, 2000; Jal *et al.*, 2004; Shen *et al.*, 2014). This process requires high energy, high-temperature, high pressure and also strong acidity (Bansal *et al.*, 2006).

Plants have natural silica synthesising system that converts water-soluble silicic acid seeped from the ground into amorphous silica by precipitation and polymerisation (Yoshida *et al.*, 1959; Lu and Hsieh, 2012). Silicon transported from the root through xylem as silicon complex are accumulated in the plants in solid form creating phytoliths (intracellular and extracellular silica bodies) (Shen *et al.*, 2014; Sivasubramanian and Kurcharlapati, 2015). A few examples of groups of plants containing natural silica are Myrtaceae, Casuarinaceae, Cyper-aceae, Gramineae, Palmae, Pinaceae, Taxodi-aceae and Equisetaceae (Shen, 2017).

Amorphous silica has been successfully extracted from rice plant, groundnut shell, sugarcane bagasse, corn cob ash, coconut shell and bamboo leaves (Rafiee *et al.*, 2012; Noushad *et al.*, 2014; Aminullah *et al.*, 2015; Sivasubramanian and Kurcharlapati, 2015; Wang *et al.*, 2015). Rice (*Oryza sativa*) which comes under the family

Gramineae, contains a high amount of silica especially in the husks (Yoshida *et al.*, 1959; Liu *et al.*, 2013). Yearly tons of RH is produced as by-products of rice, the world's second most produced crop species in countries such as China, Malaysia, Arab, Republic of Korea and India (Park *et al.*, 2003; Lu and Hsieh, 2012; Liu *et al.*, 2013). Global rice production stands around 466 million tons as of the year 2010/2011 and RH account for one-fifth of it (Rafiee *et al.*, 2012; Gu *et al.*, 2013).

One of the pioneering reports indicated the presence of amorphous hydrated silica in rice plants using FTIR analysis of untreated RH (Yoshida *et al.*, 1959). Other studies demonstrated that the sheaths contain the highest amount of silica about 17.50% in comparison to silica content in roots, stems and leaves (straw) (Lanning, 1963).

RHs has a very hard exterior surface and are mainly made up of the tightly interlocked lemma and palea, both having similar morphology. The epidermal surface of the lemma is arranged in linear ridges punctuated with prominent conical protrusions with hair like papillae extending from the surface at some intervals. The outer surface of the RHs are highly undulated and two thick layers of walls underlie the outer epidermis (Park *et al.*, 2003). Silica is heterogeneously distributed on the upper and lower surface of the RHs, in the range of micrometre-sized particle of various morphology (Bansal *et al.*, 2006). Amorphous nature of these silica makes them highly soluble and thus extractable at alkaline conditions in lower temperatures (Kalapathy *et al.*, 2002).

RH is primarily used as a fuel source and bedding for animals with limited application observed in the industrial field (Park *et al.*, 2003; Bharadwaj *et al.*, 2004). The high calorific value of RH renders it as an excellent source for heat generation and production of natural gases (Ahmed *et al.*, 2008). The primary disposal methods of RH is by burning. This causes air pollution through the release of a large number of

greenhouse gases or by stacking in farmland that wastes space (Noushad *et al.*, 2014). At the same time, RHA is also dissipated into the air causing silicosis syndrome in exposed residents (Tadjarodi *et al.*, 2012; Vaibhav *et al.*, 2015).

The hard exterior of the RH due to high silica content renders them immune to bacterial decompositions (Noushad *et al.*, 2014). The increase in the fossil fuel price has prompted the manufacturers to switch to use RH as a fuel source in industrial boilers. The burning of RH releases crystalline silica (cristobalite) into open air that is classified as a hazardous compound that causes cancer (Yang *et al.*, 2015).

Exploitation of RH for commercial purposes are being extensively explored to synthesise nanomaterial at a much lower cost. Extraction of cellulose and silica from RHA have been widely researched, to produce silica using the low-cost method from a sustainable source. This also reduces the ecological impact of accumulating RH and prevents air pollution caused by burning of this waste material (Rafiee *et al.*, 2012; Carmona *et al.*, 2013; Vaibhav *et al.*, 2015).

Silica particles synthesised from agricultural waste sources are highly porous and possesses high surface area. They are found to be a useful raw material in ceramics, electronics, catalysis, pharmaceuticals, dental materials and forensics (Choi *et al.*, 2008b; Moret *et al.*, 2014, 2016; Marin *et al.*, 2015). The composition of RH varies according to the geographical location, type of paddy, climate condition and soil chemistry. A rough composition as reported in earlier studies is summarised in **Table 2.1**.

Table 2.1 The composition of RH: Elemental and organic constituents of RH
(Soltani *et al.*, 2015)

Composition of RH	Percentage
Elemental composition	
Carbon	37.05%
Hydrogen	8.80%
Nitrogen	11.06%
Silica	9.01%
Oxygen	35.03%
Contents of RH	
Hemicellulose	24.30%
Cellulose	34.40%
Lignin	19.20%
Ash	18.85%
Others	3.25%

2.2.1 SiNP synthesis

The six routes of SiNP synthesis from synthetic precursors and RHs are vapour-phase reaction, thermal decomposition, chemical digestion, precipitation, sol-gel technique and fungus mediated transformation (Gorji and Ghasri, 2012; Noushad *et al.*, 2012; Rahman and Padavettan, 2012; Shekar *et al.*, 2012; Yue *et al.*, 2013; Moret *et al.*, 2014). Vapour-phase reaction involves an inert gas such as argon carrying the silica precursor allowing reaction with the vapour of solvents to produce SiNPs. The size of the particles can be controlled by controlling the dilution of the carrier gas (Yue *et al.*, 2013).

Thermal decomposition or chemical digestion of RHs can produce SiNPs with various purity levels (Hanafi, 1980; James and Rao, 1986; Conradt *et al.*, 1992; Krishnarao *et al.*, 2001). The sol-gel process utilises soluble molecular precursors transformed into atomic seeds of an element and followed by polymerisation or condensation subsequently forming larger particles (Coradin *et al.*, 2006). Precipitation of SiNP from sodium silicate generated from RH (SS_{th}) solution can also be realised by inhibiting gel growth and promote polymerisation to form silica powders. Conditions

of the precipitation may be altered by the addition of solvents, change in pH or by creating microemulsion state to control particle growth (Jal *et al.*, 2004).

Reverse microemulsion or water-in-oil microemulsion method can be defined as a thermodynamically stable and transparent solution containing water, oil and surfactant. The solution contains tiny micelles or droplets of nanosized water entities dispersed in oil. Surfactant functions to form a barrier like a wall around the liquid droplets creating nanosize reactor wells that allow limited reaction of nanoparticle formation and avoids molecular aggregation (Bagwe *et al.*, 2004; Naka *et al.*, 2010).

Another synthesis method is the combustion of precursors in the form of gas, liquid and solid which are injected into the burner and instantaneously reacted at high-temperature to form product molecules. This molecule then undergoes subsequent reactions and finally coalesce to form larger aggregates (Shekar *et al.*, 2012; Yue *et al.*, 2013). RH can also be digested using certain fungus to extract and transform amorphous silica into a crystalline state (Bansal *et al.*, 2006).

As a greener alternative, high content of silica in RH have been exploited and explored as a possible source for SiNP, silicon carbide, silicon nitride, sealon and zeolite synthesis (Noushad *et al.*, 2012, 2014; Gu *et al.*, 2013; Zulkifli *et al.*, 2013; Shen *et al.*, 2014; Marin *et al.*, 2015). Over the years, more studies have been centred on the optimisation of each governing parameters of SiNP production from RH. Copious studies have been undertaken to produce purer silicon compounds by acid and alkali leaching as well as modulating RH sintering temperatures (Kalapathy *et al.*, 2000, 2002; Della *et al.*, 2002; Zaky *et al.*, 2008).

Extraction and purification of silica from RH must be tailored to the intended use of the product. SiNP can be extracted in three forms; crystals, gels and powder.

Modifying the stability of the solution by controlling the electrical charges can be used to modulate the final form of the SiNP. Polymerisation or repulsion of particles can be fluctuated by decreasing or increasing the surface charges respectively. Various parameters such as pH and solvents can be used to alter the electrical charges resulting in the formation of SiNP of different characteristics (Le *et al.*, 2013).

2.2.1 (a) Extraction of SiNP through thermal decomposition of RH

The crudest form of silica with low purity can be extracted by thermal treatment of RH. Burning the RH at elevated temperature is undoubtedly the easiest method to extract silica. However, the side effects of the method such as pollution have induced scientists to implore a relatively benign manner of silica extraction (Adam *et al.*, 2011; Zulkifli *et al.*, 2013). The burning of RH at 450°C or above retains the trace metal impurities that interfere with the final characteristics of the amorphous silica (Lu and Hsieh, 2012). The presence of trace metal impurities affects the purity of the silica, causes surface melting and crystallisation of silica during heat treatment and also carbon fixation in RHA. Quality, colour and state of the RHA are dependent on factors such as pretreatment with chemicals, ashing temperature and heating rate (Rafiee *et al.*, 2012).

RHA with different levels of purity and crystallisation can be obtained by modulating the heating rate and temperature as well as chemical pre-treatment. Physicochemical changes of the RH after chemical and heat treatments can be monitored using analytical instruments such as surface area analyser, XRD, dynamic thermoanalytical techniques and FTIR (James and Rao, 1986). RHA which mainly contains silica can be produced when RH is heated at a high temperature above 500°C. The increasing and decreasing pattern in the total surface area together with the crystallinity of the

RHA as the heating temperature was increased from 500 to 1400°C offers insight into the morphological changes RH undergoes (Hanafi, 1980).

Total surface area of the RHA increased when heating temperature was increased from 500 to 600°C, indicating break down of silica into SiNP. Then a decreasing trend was observed when the temperature was further increased to 900°C, representing either agglomeration of the smaller particles or size growth (Ibrahim and Helmy, 1981). A sudden plunge in the total surface area and change in crystalline state can be observed at a heating temperature beyond 900°C indicating amorphous silica began crystallising (Vaibhav *et al.*, 2015). Further increase in heating temperature beyond 1400°C leads to a sudden increase in the surface area indicating the formation of smaller crystals (Hanafi, 1980; Fernandes *et al.*, 2017).

Thermal decomposition analysis sheds light on the chemical changes that RH undergoes as the thermal treatment is conducted. Three major decomposition peaks at 373K, 533K and 735K can be observed during the heat treatment of RH. The first peak was attributed to the loss of sorbed water (James and Rao, 1986). The second major mass loss was attributed to the breakdown of the cellulose and lignin constituents through glowing combustion (Liou, 2004; Fernandes *et al.*, 2017) and the final exotherm indicated combustion of product gases or from lignin decomposition as postulated by another researcher (Abu *et al.*, 2016).

A complete combustion was favoured in an oxygenated atmosphere in comparison to the nitrogen-saturated atmosphere (James and Rao, 1986). Heating RH or black RHA obtained from rice mill at 500°C for 8 hours or at 700°C for 6 hours produced white amorphous RHA with 94.95 % purity but with drastic decrease in total surface area

from 177 m²/g to 54 m²/g after heat treatment owing to the agglomeration effect and diminished porosity (Della *et al.*, 2002).

Silica of higher purity can be extracted from RH by removal of the trace metal impurities using chemical treatment pre or post to heating treatment. Volumes of research have been dedicated to determining the optimal type and concentration of the chemical for RH treatment as well as the duration of chemical and heat treatment. The treatment was aimed to produce pure SiNP with small size and high surface area. To date, the literature shows consensus on pre-treatment of RH using hydrochloric acid (HCl) before heat treatment to produce the purest silica possible with the highest surface area and smallest size. Prior to reaching this conclusion, various other chemicals have been tested for the chemical treatment of RH to completely remove trace metal impurities. HCl, nitric acid, sulphuric acid and NaOH were among the chemicals tested for this purpose (Mishra *et al.*, 1985; Chakraverty *et al.*, 1988; Conradt *et al.*, 1992; Abu *et al.*, 2016).

Pre-treatment of RH using NaOH did not only remove trace metal impurities but also silica. This was due to amorphous silica has a high solubility in alkali medium (Conradt *et al.*, 1992). Treatment of RH using boiled solutions of HCl, sulphuric acid, phosphoric acid, nitric acid and other acid is effective in breaking down cellulose and lignin components as well as removing metallic impurities. Acid component reacts with the metal to form soluble compounds that can be washed out from the solid residue (Sun and Gong, 2001).

Previous findings have reported that HCl pre-treated RH produces silica of the highest purity of approximately 99.86% after heat treatment followed by sulphuric and nitric acid pre-treated RH at approximately 99% purity (Yalçin and Sevinç, 2001; Wang *et*

al., 2012; Ghorbani *et al.*, 2015; Abu *et al.*, 2016). Theoretically, the nitric acid should be able to remove trace metal impurities effectively in comparison to HCl because metal nitrates are more soluble than metal chlorides (Speight, 2005). However, in this case, HCl was reported to be more effective in removing trace metal impurities than nitric acid. This might be because nitric acid reacts with cellulose present in the RH forming nitrocellulose reducing its reactivity with trace metals (Baumann *et al.*, 1982). HCl does not react with cellulose but helps with acid hydrolysis of cellulose into oligosaccharides (Fan *et al.*, 1987).

Another study claimed that production of highly pure RHA was possible by subjecting raw RHA formed from combusting RH at 500°C to acid treatment for two hours. However, the authors did not conduct an elemental analysis of the product to support their claim (Mishra *et al.*, 1985). This finding was not in agreement with a later report which stated that the RHA produced without prior acid treatment remained light brown concurrent with other subsequent research (Chakraverty *et al.*, 1988; Real *et al.*, 1996). A dramatic drop in the total surface area occurred if the acid leaching was conducted after ashing. This phenomenon was attributed to the interaction of potassium ion and silica. Potassium ion causes surface melting when RH was subjected to sudden heating trapping the carbon particles in the ashes (Krishnarao *et al.*, 2001; Rafiee *et al.*, 2012).

The ash produced retained the shape of the RH grains when viewed under SEM but soft grinding of the ash results in a fine powder (Liou, 2004). This further offered to prove that silica was homogeneously distributed on the surface of RH since the ash contains 99% \pm silica. The fine silica ash observed under SEM revealed SiNP smaller than 100 nm whereby the particles exhibited a high level of agglomeration (Conradt *et al.*, 1992).